X-ray Rich GRB, Photospheres and Variability

P. Mészáros [1,2], E. Ramirez-Ruiz[3], M. J. Rees[3] & B. Zhang[1]

[1]Dpt. of Astronomy & Astrophysics, Pennsylvania State University, University Park, PA 16803
[2]Dpt. of Physics, Pennsylvania State University, University Park, PA 16803
[3]Institute of Astronomy, University of Cambridge, Madingley Road, Cambridge CB3 0HA, U.K.

ApJ, submitted: 5/8/02; accepted: 6/20/02

ABSTRACT

We investigate the relationship between the quasi-thermal baryon-related photosphere in relativistic outflows, and the internal shocks arising outside them, which out to a limiting radius may be able to create enough pairs to extend the optically thick region. Variable gamma-ray light curves are likely to arise outside this limiting pair-forming shock radius, while X-ray excess bursts may arise from shocks occurring below it; a possible relation to X-ray flashes is discussed. This model leads to a simple physical interpretation of the observational gamma-ray variability-luminosity relation.

Subject headings: gamma-rays: bursts – shock waves – X-rays: bursts

1. Introduction

Gamma-ray burst (GRB) light curves at γ-ray energies are often highly variable, and generally this is attributed to internal shocks occurring at some radius $\gtrsim 10^{12} - 10^{14}$ cm from the center of a relativistic outflow produced by a violent collapse or merger, beyond the "photospheric" radius at which the flow becomes optically thin to scattering by electrons associated with the baryons entrained.

This photosphere is a source of soft thermalized radiation, which may be observationally detectable in some GRB spectra, and may also result in inverse Compton cooling of the non-thermal electrons accelerated in the shocks occurring outside it, thereby enhancing a hard GeV non-thermal component at the expense of the usual MeV synchrotron component.

At small enough radii, however, the shocks can create enough pairs to re-establish a second photosphere caused by the pairs, and it is only beyond a limiting radius that the shocks remain optically thin to pairs. The most favorable region for shocks producing highly variable gamma-ray light curves is above this radius, while shocks occurring below it would lead to a second source of less variable radiation (Kobayashi, Ryde & MacFadyen 2002; see also Ramirez-Ruiz &

Lloyd-Ronning 2002; and Spada, Panaitescu & Mészáros 2000), which is also X-ray rich. Bursts dominated by either the baryonic photosphere or by pair-producing shocks may be identified with X-ray excess bursts (Preece *et al.* 1996), while the latter resemble at least the harder examples of the proposed X-ray flash (Heise *et al.* 2001) sub-class of GRB.

The existence of a limiting pair-forming shock radius provides also a scenario which combines recent work on the interpretation of afterglow light-curve breaks in terms of a jet opening angle (Frail *et al.* 2001; Panaitescu & Kumar 2001; Piran *et al.* 2002) or a universal jet shape (Rossi, Lazzati & Rees 2002; Zhang & Mészáros 2002; Salmonson & Galama 2002), and work on the gamma-ray variability-luminosity relationship (Fenimore & Ramirez-Ruiz 2001; Reichart *et al.* 2001). Identifying the pair shock radius as an approximate boundary above which shocks lead to more strongly variable gamma-ray light curves and below which shocks result in smoother X-ray rich light curves, a phenomenological jet model leads to a simple physical explanation of the quantitative form of the variability-luminosity relationship.

2. Baryonic Photospheres

Consider a relativistic wind outflow where the bulk Lorentz factor has a mean dimensionless entropy $\eta = L_o/\dot{M}c^2 = 10^2\eta_2$ which varies ($\Delta\eta \sim \eta$) on timescales t_v ranging from a minimum dynamical timescale up to the maximum burst (wind) duration t_w, $10^{-3}\ s \leq t_v \lesssim t_w$. The flow starts from a minimum radius $r_o = ct_{v,min} = 10^7 r_{o,7}$ cm, and the Lorentz factor accelerates as $\Gamma \propto r$ up to a coasting (or saturation) radius $r_c \sim r_o\Gamma_f$, beyond which it coasts as $\Gamma = \Gamma_f$. For a simple wind, neglecting finite shell effects, $\Gamma_f = \min[\eta, \eta_*]$ where the value η_* is a critical value of the dimensionless entropy given by (Mészáros & Rees 2000)

$$\eta_* \simeq \ell_{p,o}^{1/4} = (L_o\sigma_T/4\pi m_p c^3 r_o)^{1/4} \simeq 10^3 (L_{52} r_{o,7}^{-1})^{1/4}\ . \tag{1}$$

Here $\ell_{p,o}$ is analogous to the definition of the compactness parameter but using the proton instead of the electron mass. The coasting Γ_f values follow from the criterion that the proton drag time must be longer than the expansion time for protons to start to coast. Below the baryonic photosphere protons are naturally coupled to radiation, but in the optically thin region above the photosphere, if this occurs in the accelerating regime, the protons can still coupled to radiation and continue to accelerate out to a radius beyond the photosphere. The comoving density in the (continuous) wind regime is $n' = (L_o/4\pi r^2 m_p c^3 \eta\Gamma)$, and using the above behavior of Γ below and above the coasting radius, as well as the definition of the Thompson optical depth in a continuous wind $\tau_T \simeq n'\sigma_T(r/\Gamma)$ we find that the baryonic photosphere where $\tau_T = 1$ in the wind (w) regime, due to electrons associated with baryons, is

$$\frac{r_{ph,w}}{r_o} = \begin{cases} \eta_*^{4/3}\eta^{-1/3} & \text{for } r < r_o\eta; \\ \eta_*^4\eta^{-3} & \text{for } r > r_o\eta, \end{cases} \tag{2}$$

where for a wind $r_c \equiv r_o \min[\eta, \eta_*]$ is the coasting radius beyond which $\Gamma = \Gamma_f =$ constant.

The accelerating and coasting behavior is followed on average also if the outflow consists of shells of duration $t_v = \Delta_o/c \geq r_o$, separated by intervals which could similarly be of order $\sim t_v$ (or a superposition of several such frequencies), leading to an oscillatory modulation of the linear and coasting behavior. Aside from such modulation, in the optically thick regime the Lorentz factor can never exceed $\Gamma \leq \eta$. However taking into account the finite shell structure, in the optically thin regime the coasting Γ_f will differ for some η from the values $\min[\eta, \eta_*]$ discussed in the wind problem. Taking for simplicity shells resulting from the minimum variation timescale $\Delta_o = ct_{v,min} = r_o$, the evolving comoving width of the shell is $\Delta' = [r,\ r_o\eta,\ \eta^{-1}r]$ and the comoving volume of the shell is $V' = 4\pi r^2\Delta' = [4\pi r^3,\ 4\pi\eta r_o r^2,\ 4\pi\eta^{-1}r^3]$ when r is $[< r_o\eta,\ \ > r_o\eta,\ \ > r_o\eta^2]$. The comoving particle density $n' = (Lt_v/\eta m_p c^2 V')$ and the Thomson depth $\tau_T = n'\sigma_T\Delta' = 1$ define a baryonic photosphere in the discrete shell (ds) regime

$$\frac{r_{ph,ds}}{r_o} = \eta_*^2\eta^{-1/2} \quad \text{for both } r < r_o\eta \text{ and } r > r_o\eta \ . \tag{3}$$

For a wind made up of shells of approximate duration t_v ejected at intervals of order t_v, at high η the shells move fast enough that a photon arising in one shell never crosses more than that one shell. At lower η, however, a light ray can cross many shells before escaping, and the appropriate expression for the photosphere approximates that of the wind equation (2). The criterion for the latter to be valid is that $r \lesssim \Delta_o\eta^2 = r_o\eta^2$, and the transition occurs at $\eta = \eta_t$ given by

$$\eta_t = \eta_*^{4/5} = 2.5 \times 10^2 (L_{52} r_{o,7}^{-1})^{1/5} \tag{4}$$

Thus one has for the baryonic photosphere

$$\frac{r_{ph}}{r_o} = \begin{cases} \eta_*^4\eta^{-3} = \eta_t^5\eta^{-3} & \text{for } \ \eta \leq \eta_t; \\ \eta_*^2\eta^{-1/2} = \eta_t^{5/2}\eta^{-1/2} & \text{for } \eta > \eta_t, \end{cases} \tag{5}$$

where the first (wind regime) occurs only in the coasting regime, while the second (shell regime) applies partly in the accelerating and partly in the coasting regimes. These regimes differ from those in Mészáros & Rees (2000) by having a break at $\eta_t = \eta_*^{4/5}$ instead of η_*, and by having a slope -1/2 above η_t instead of -1/3 (due to the shell regime, neglected in our previous paper). The photosphere is in the coasting wind regime for $\eta \leq \eta_t$, in the coasting shell regime for $\eta_t \leq \eta \leq \eta_*^{4/3}$, and in the accelerating shell regime for $\eta \geq \eta_*^{4/3}$ (see Fig. 1). When the photosphere is above the coasting radius, the final Lorentz factor is just $\Gamma_f \sim \eta$. When the photosphere is below the coasting radius, the baryons continue to be dragged by the radiation above the photosphere until $t'_{drag} \sim (m_p c^2/c\sigma_T u'_\gamma)$ exceeds $t'_{exp} \sim r/c\Gamma$, out to a radius $r_{drag}/r_o \leq \eta_*^2$ where $\Gamma \sim \min[\eta_*^2\eta^{-1/2}, \eta_*]$. The final Lorentz factor is thus $\Gamma_f = [\eta, \eta_*^2\eta^{-1/2}, \eta_*]$ for values of $[\eta < \eta_*^{4/3},\ \eta_*^{4/3} < \eta < \eta_*^2,\ \eta > \eta_*^2]$. This results in shock radii (Figure 1) which are divided into three regimes (instead of the two in Mészáros & Rees 2000, where in the wind regime the values η_t and $\eta_*^{4/3}$ were collapsed into a single η_*).

In units of the initial total luminosity L_o and initial temperature at r_o, $\Theta_o = kT_o/m_e c^2 \simeq 2L_{52}^{1/4} r_{o,7}^{-1/2}$ (i.e. $T_o \sim 1\ L_{52}^{1/4} r_{o,7}^{-1/2}$ MeV), the lab-frame baryonic photospheric

luminosity L_{ph} and dimensionless temperature Θ_{ph} behave as

$$\frac{L_{ph}}{L_o} = \frac{\Theta_{ph}}{\Theta_o} = \begin{cases} (r_{ph}/r_c)^{-2/3} = (\eta/\eta_*)^{8/3} = \eta_t^{-2/3}(\eta/\eta_t)^{8/3} & \text{for } \eta < \eta_t; \\ (r_{ph}/r_c)^{-2/3} = \eta_*^{-1/3}(\eta/\eta_*) = \eta_t^{-2/3}(\eta/\eta_t) & \text{for } \eta_t < \eta < \eta_*^{4/3}; \\ 1 & \text{for } \eta > \eta_*^{4/3}. \end{cases} \quad (6)$$

Thus $(L_{ph}/L_o) = (\Theta_{ph}/\Theta_o) = \eta_*^{-8/15} = 2.5 \times 10^{-2}$ ($T_{ph} \sim 25/(1+z)$ keV in the observer frame) for $\eta = \eta_t = \eta_*^{4/5} \sim 250$; $(L_{ph}/L_o) = (\Theta_{ph}/\Theta_o) = \eta_*^{-1/3} = 10^{-1}$ for $\eta = \eta_* = 10^3$; and $(L_{ph}/L_o) = (\Theta_{ph}/\Theta_o) = 1$ at $\eta = \eta_*^{4/3} \sim 10^4$ (where the photosphere occurs at the coasting radius).

The internal shocks, which occur in the coasting regime at radii $r/r_o = (\Delta_o/r_o)\eta^2 \geq \eta^2$, produce a shock photon luminosity

$$L_{sh} = \epsilon_e \epsilon_i L_o \sim 10^{-1} \epsilon_{e,1/3} \epsilon_{i,1/4} L_o \ , \quad (7)$$

where the shock efficiency $\epsilon_{sh,-1} = 10^{-1}\epsilon_{e,1/3}\epsilon_{i,1/4}$ is a bolometric radiative efficiency when the cooling timescale is shorter than the dynamical time. Similarly the magnetic luminosity (if the turbulent field energy $\epsilon_B = (1/3)\epsilon_{B,1/3}$ is in equipartition with that of randomized protons and electrons) is $L_B = \epsilon_B \epsilon_i L_o \sim 10^{-1}\epsilon_{B,1/3}\epsilon_{i,1/4} L_o \simeq L_{sh}$. Thus, $L_{ph} \ll L_{sh} \sim L_B$ for $\eta < \eta_t \sim 250$; $L_{ph} < L_{sh} \sim L_B$ for $\eta_t < \eta < \eta_* \sim 10^3$; and $L_{ph} > L_{sh} \sim L_B$ for $\eta_* < \eta < \eta_*^{4/3} \sim 10^4$. This means that for $\eta > \eta_* \sim 10^3$ the baryonic photospheric component dominates the non-thermal internal shock component in a bolometric sense. This will lead to inverse-Compton cooling of the non-thermal electrons accelerated in the shocks, causing a weakening and softening of the nonthermal synchrotron spectrum of the shock, at the expense of a hard ($\gtrsim$ GeV) inverse Compton component, while most of the energy will be in a thermal X-ray component.

The BATSE γ-ray luminosity is broad-band in nature, and can be written as $L_\gamma \sim (1/5)(1-\epsilon_{IC})L_{sh} \lesssim (1/5)L_{sh}$ where ϵ_{IC} is the IC efficiency, with a peak synchrotron frequency depending on the comoving magnetic field value B'. For low values of η, shocks occur closer in, leading to higher B' and harder synchrotron peaks. For $\eta \sim \eta_t$ the baryonic thermal X-ray photosphere may be responsible for the X-ray excess BATSE bursts (Preece *et al.* 1996). For lower η the photospheric thermal peak is even softer, while the shocks occur closer in and produce harder synchrotron peaks approaching the upper, less sensitive end of the BATSE band, which could lead to an apparent dominance of the soft X-ray thermal photospheric peak.

For higher values $\eta_t \lesssim \eta \lesssim \eta_*$ the thermal peak tends to blend with the synchrotron peak, resembling the canonical non-thermal GRB spectrum, while for $\eta \gtrsim \eta_*$ a hard ($\gtrsim$ MeV) thermal component would be predicted to dominate.

3. Shocks Above the Pair-Radius and Variable γ-ray lightcurves

When shells of mass $(m/2)$ with Lorentz factors Γ_1 and Γ_2 collide, the mechanical efficiency for conversion of kinetic energy $mc^2(\Gamma_1+\Gamma_2)$ into internal energy is $\epsilon_i = (\Gamma_1+\Gamma_2-2\sqrt{\Gamma_1\Gamma_2})/(\Gamma_1+\Gamma_2)$,

where as before we parameterize $\epsilon_i = (1/4)\epsilon_{i,1/4}$. If a total of $2N$ shells are ejected which collide, and the total isotropic equivalent kinetic energy of outflow is E_{iso}, the corresponding internal energy produced in the merger of two shells is $E_{int} \sim \epsilon_i N^{-1} E_{iso}$. Of that, a fraction ϵ_e is given to electrons, and for a high radiation efficiency in the MeV range and a high compactness parameter (i.e. high efficiency of pair formation) a fraction of order 1/3 of the radiated energy could be converted into pairs, and the energy in pairs in the merged shell is

$$E_{\pm} \sim \epsilon_e \epsilon_i (1/3N) E_{iso} \sim 10^{50.5} \epsilon_{e,1/3} \epsilon_{i,1/4} N_2^{-1} E_{54} \text{ erg.} \tag{8}$$

Assuming that Γ in in the range $[\Gamma_m, \Gamma_M]$, with $\Gamma_m < \Gamma_M$, the observed radiation comes mainly from collisions involving shells at the extremes of this range and is maximized for $\Gamma_m \ll \Gamma_M$. Such merged shells move with a center of mass Lorentz factor $\Gamma_c \sim \sqrt{\Gamma_m \Gamma_M}$. For shells of initial lab-frame widths $\Delta_o \sim r_o$, for radii above the shock radius $r_{sh} = r_o \eta^2$ (which is also the "expansion radius" above which the comoving width $\propto r$ and the comoving volume $\propto r^3$) the energy radiated in the shocks can be enough to create pairs which make the shocked shells optically thick to Thomson scattering, if η is below a certain value for which the comoving radiation compactness parameter $\ell' \sim (L\sigma_T / m_e c^3 r) \gtrsim 1$ (Mészáros & Rees 2000). Earlier simulations involving randomly ejected shells and (baryonic) electron scattering in shocks have indicated a tendency for more variable light curves arising in more distant shocks (Panaitescu *et al.* 2000; Spada *et al.* 2000; Ramirez-Ruiz & Lloyd-Ronning 2002), as expected since closer in the scattering depth is larger. Similar results are obtained numerically when pair formation is included, e.g. Kobayashi *et al.* (2002). Here we pursue a simplified analytical description. For shocks at increasing radii, the pair comoving scattering depth of the shells eventually drops to unity, $\tau'_{\pm} \sim n'_{\pm} \sigma_T (r/\Gamma_c)$ $\sim (E_{\pm} \sigma_T / 4\pi r^2 \Gamma_c) \sim 1$ at a characteristic limiting pair-producing shock radius

$$r_{\pm} \sim (E_{\pm} \sigma_T / 4\pi m_e c^2 \Gamma_c)^{1/2} \sim 3 \times 10^{14} (\epsilon_{e,1/3} \epsilon_{i,1/4} N_2^{-1} E_{54})^{1/2} (\Gamma_{M,3} \Gamma_{m,2})^{-1/4} \text{ cm,} \tag{9}$$

(Kobayashi *et al.* 2002) where $\Gamma_m = 10^2 \Gamma_{m,2}$, $\Gamma_M = 10^3 \Gamma_{M,3}$. This is in the discrete shell regime, as opposed to the wind regime used Mészáros & Rees 2000; in general the shell regime pair density exceeds the wind regime pair density by a factor $(t_w/t_v N)(\Gamma_c/\Gamma_m)^2 \geq 1$, as expected since the same kinetic energy density is concentrated in shells rather than smoothed out. At this radius both the comoving scattering time and the pair formation time as well as the comoving pair annihilation time $(n'_{\pm} \sigma_T c)^{-1}$ become equal to the comoving expansion time $r_{\pm}/c\Gamma_c$.

Shells with Lorentz factors Γ_M and Γ_m ejected from a starting radius r_o at time intervals $t_v = \Delta_o/c$ collide at a radius $r_{sh} \sim c t_v \Gamma_m^2 \gtrsim r_o \eta^2$. If this shock radius is outside the limiting pair-shock radius $r_{\pm}$ given by equation (9), pairs do not form in the shock, whereas in the opposite case an optically thick pair region does form in the merged shell, which expands until it reaches the radius $r_{\pm}$. The shocks which occur outside the limiting pair-shock radius $r_{\pm}$ are those for which the corresponding shells started out from r_o with a minimum time difference $t_v > t_{v\pm}$, where

$$t_{v\pm} \sim r_{\pm}/c\Gamma_c^2 \sim 0.2 (\epsilon_{e,1/3} \epsilon_{i,1/4} N_2^{-1} E_{54})^{1/2} \Gamma_{M,3}^{-5/4} \Gamma_{m,2}^{-5/4} \text{ s.} \tag{10}$$

If the shell ejection time differences t_v have random realizations between the minimum and maximum values $[t_{v,m}, t_{v,M}]$ over the total duration of the burst outflow $t_b \gtrsim t_{v,M}$, out of the N shells ejected there will be, on average, a fraction $(1 - t_{v\pm}/t_{v,M})$ which will lead to shocks outside the pair-shock radius. For a high radiative efficiency, a fraction $0.5\epsilon_{\gamma,1/2}$ of which is taken to be in the gamma-ray range, the isotropic-equivalent gamma-ray fluence of the shocks above the limiting pair-shock radius is approximately

$$E_\gamma \sim (1/2)\epsilon_{\gamma,1/2}\epsilon_e\epsilon_i E_{iso}\left(1 - \frac{t_{v\pm}}{t_{v,M}}\right) \sim 4\times 10^{52}\epsilon_{\gamma,1/2}\epsilon_{e,1/3}\epsilon_{i,1/4}E_{54}\left(1 - \frac{t_{v\pm}}{t_{v,M}}\right)\ \text{erg}. \qquad (11)$$

Here $t_{v\pm}/t_{v,M} \sim 2\times 10^{-2}(\epsilon_{e,1/3}\epsilon_{i,1/4}N_2^{-1}E_{54})^{1/2}t_{b,1}^{-1}\Gamma_{M,3}^{-5/4}\Gamma_{m,2}^{-5/4} \lesssim 1$, with $t_{v\pm} \lesssim t_{v,M} \lesssim t_b$ where $t_b = 10t_{b,1}$ s is the burst duration. In this simple model E_γ represents the energy in the variable γ-ray component of the burst, which arises above $r_\pm$ and has variability on timescales $\gtrsim t_{v\pm}$. For $t_{v\pm} \ll t_b$, E_γ is insensitive to Γ_m, but for short bursts or for $t_{v\pm} \gtrsim 0.1t_b$ there is a dependence of E_γ on $t_{v\pm} \propto \Gamma_m^{-5/4}$. For small Γ_m the typical pair-shock radius $r_\pm$ is further out, and the minimum variability timescale $t_{v\pm}$ is longer, with a consequently smaller variable E_γ (fewer shocks occur outside the more distant limiting pair-shock radius). Larger Γ_m lead to smaller limiting pair-shock radii, shorter minimum variability timescales $t_{v\pm}$ and larger isotropic equivalent E_γ.

4. Pair-producing Shocks and X-ray Rich Component

For shocks occurring at $r_{sh} \leq r_\pm$, i.e. below the limiting pair-shock radius where shocks can result in pair formation, the scattering optical depth of the shocked shells can become $\tau'_\pm \gtrsim 1$ (even when the shock is above the baryonic photosphere given by equations [2,3]). Pair formation causes the same amount of shock energy to be spread among a larger number of particles (new pairs) than in a purely baryonic outflow, and inverse Compton losses due to up-scattering of its own photons (Ghisellini & Celotti 1999) become important. For a pair of shells undergoing a shock at $r < r_\pm$, it is expected that pair-production acts as a thermostat, and for comoving compactness parameters $10 \lesssim \ell' \lesssim 10^3$ the comoving pair temperature is $T'_\pm \sim 3 - 30$ keV, with $\tau'_\pm \sim$ few (Svensson 1987). The scattering depth per shock due to pairs is unlikely to be much larger, because the scattering and the pair-formation cross sections are comparable, and unless dissipation and pair formation occurs uniformly throughout the entire volume, down-scattering of photons above the pair threshold rapidly leads to self-shielding (Ramirez-Ruiz *et al.* 2002). As a specific example, we take $T'_\pm \sim 10$ keV and $\tau'_\pm \sim 3$ for one shock, producing a comoving spectrum peaked near $h\nu' \sim 3kT'_\pm/\tau'^2_\pm \sim 3T'_{\pm,10}\tau'^{-2}_{\pm,3}$ keV. Since at any time there may be more than one shock at $r < r_\pm$, the photons might encounter more than one shell before escaping (e.g. Spada *et al.* , 2000), and would also undergo adiabatic cooling between the shells by a factor $\sim r_{sh}/r_\pm$. These two effects combined could lower the escaping photon energy by a factor roughly estimated as $\zeta \sim 0.2\zeta_{0.2}$. For a CM bulk Lorentz factor $\Gamma_c = (\Gamma_M\Gamma_m)^{1/2} = 300\Gamma_{c,2.5}$, the observer-frame

pair-producing shock radiation peak is at

$$h\nu_{x,sh} \sim 100\ T'_{\pm,10}\tau'^{-2}_{\pm,3}\zeta_{0.2}\Gamma_{c,2.5}[2/(1+z)]\ \mathrm{keV}\ . \tag{12}$$

The peak energy (12) is still substantially above the black-body value $T_{sh,BB} \sim 4\ (\epsilon_{e,1/3}\epsilon_{i,1/4}E_{54}N_2^{-1})^{-1/8}\Gamma_{c,2.5}^{11/8}$ keV. The BATSE distribution of peak energies (Preece *et al.* 2000) has $\sim 10\%$ of bursts with $h\nu_{pk} \lesssim 100$ keV, while the joint BATSE-BeppoSAX distribution of Kippen *et al.* (2002) shows that most X-ray flashes (XRF) have peak energies in the 20-100 keV range, with one exception at 3^{+4}_{-3} keV. A nominal value of $h\nu_{pk} \sim 20$ keV can be obtained from equation (12) with, e.g. $\Gamma_c[2/(1+z)] \sim 60$

For completeness, we note that in the extreme case where pairs are produced uniformly throughout the entire volume, thermalization and an equilibrium pair optical depth $\tau'_\pm \propto \ell'^{1/2}$ might be achieved, where ℓ' is the comoving compactness (Guilbert, Fabian & Rees 1984; Svensson 1987), although we expect $\tau_\pm$ in this case to be much smaller.

The energy in the X-ray component from shocks arising below the limiting pair-shock radius $r_\pm$, integrated over the burst duration t_b, is the complement of the γ-ray energy produced in shocks arising above $r_\pm$ [c.f. equation (11)]. The X-ray isotropic equivalent fluence is

$$E_x \sim (1/2)\epsilon_k\epsilon_e\epsilon_i E_{iso}\left(\frac{t_{v\pm}}{t_{v,M}}\right) \sim 4\times 10^{50}\epsilon_{k,1/2}(\epsilon_{e,1/3}\epsilon_{i,1/4}E_{54})^{3/2}N_2^{-1/2}t_{b,1}^{-1}\Gamma_{M,3}^{-5/4}\Gamma_{m,2}^{-5/4}\ \mathrm{erg}, \tag{13}$$

where $t_{v\pm}/t_{v,M}$ is given below equation (11), $\epsilon_k = (1/2)\epsilon_{k,1/2}$ is an efficiency factor to account for a fraction of order unity of the luminosity below $r_\pm$ which is re-converted into kinetic energy. This X-ray component could account for most of the harder X-ray flashes (Heise *et al.* 2002; Kippen *et al.* 2002), with $h\nu_{pk} \gtrsim 20$ keV, but if more XRFs are observed with peaks as low as 3-5 keV this may require additional considerations. On the other hand, the X-ray excess GRB discussed by Preece *et al.* (1996) have characteristics which, as a class, are close to those of the $r_{sh} \lesssim r_\pm$ pair-producing shocks discussed in this section.

The radiation from pair-shocks with $\tau_\pm \sim$ few would be subject to a moderate amount of time-smoothing $\Delta t_{var} \sim \Delta t_{var,orig}\tau_\pm$, which partially degrades the original variability implied by the random ejection and shocking of shells. The smoothing would be more appreciable at the shorter timescales, where it would lead to a filling in of the narrow troughs between peaks (see also Panaitescu *et al.* 2000; Kobayashi *et al.* 2002 and Ramirez-Ruiz & Lloyd-Ronning 2002). This smoothing, however, would not be expected to affect the coarser time structure of the light curve, since not many scatterings are incurred before the photons are advected with the flow.

5. Variability Dependence on γ-ray Luminosity

An observational correlation (Fenimore & Ramirez-Ruiz 2001; Reichart, *et al.* 2001) has been reported between the isotropic equivalent luminosity L_γ and a variability measure V of the γ-ray

time profiles, of the form

$$L_\gamma \propto V^g, \quad \text{where} \quad g \simeq 3.3^{+2.5}_{-1.1} \ . \tag{14}$$

The operational definition of V is related to the normalized variance, or the root mean square of the deviations from a smoothed light curve. Observations of afterglows with breaks in the light curves are believed to indicate the presence of a collimated jet-like outflow. The simplest interpretation assumes a uniform jet cross-section (independent of angle out to a jet edge θ), in which case the variety of break times indicates a variety of jet opening angles and the data indicate an isotropic equivalent fluence anti-correlation with jet opening angle θ (Frail *et al.* 2001), of the form $L_{\gamma,iso} \propto \theta^{-2}$. Alternatively, the same data can be interpreted in terms of a non-uniform (angle-dependent) cross section jet with a universal jet pattern given by the same functional relation between the energy output as a function of angle $L_\gamma(\theta) \propto \theta^{-2}$ (Rossi *et al.* 2002; Zhang & Mészáros 2002; Salmonson & Galama 2002). In the latter case the data is interpreted as sampling different off-sets between the observer line of sight and the jet axis. Norris (2002) and Salmonson & Galama (2002) analyzing the time-lag effects (see below) in a larger sample and including redshift and luminosity function effects, argue for a somewhat steeper angular index of -5/2, so

$$L_\gamma \propto \theta^{-p}, \quad \text{where} \quad p \sim 2 - 2.5 \ . \tag{15}$$

In the previous sections we used an isotropic outflow but our results continue to apply to the jet case as long as Γ exceeds the inverse of the jet opening angle θ. The model interprets the variable γ-ray luminosity as that portion which arise from shocks above the limiting pair-shock radius $r_\pm$, characterized by a minimum time variability given by equation (10), $t_{v\pm} \propto L_\gamma^{1/2}\Gamma_m^{-5/4}$. This is based on equation (11) relating $E_{\gamma,iso} \sim E_\gamma$ to E_{54}, and the assumption that the average mean duration and redshift differences are overshadowed by source-intrinsic variations in E_γ and Γ_m, so that approximately $L_\gamma \propto E_\gamma$, and assuming that $t_{v\pm} \ll t_{v,M}$. The crucial dependence of $t_{v\pm}$ is through Γ_m, rather than Γ_M, since it is Γ_m which determines the shock radius. It is reasonable to make the ansatz $\Gamma_m \propto \theta^{-q}$, and a value $q \sim 2$ (e.g. MacFadyen & Woosley 1999; Kobayashi *et al.* 2002) follows from momentum conservation in a "sharp boundary jet" model where the energy and Γ are constant throughout its cross section but there is a range of opening angles (e.g. Frail *et al.* 2001). In a "universal jet profile" model where L and Γ vary as function of θ (Rossi *et al.* 2002; Zhang & Mészáros 2002; Salmonson & Galama 2002), a value $q \sim 2$ is also expected, e.g. if the baryon loading in the jet are approximately independent of θ but the energy varies as θ^{-2} (e.g equation [15]). Setting $\Gamma_m \propto \theta^{-q}$, we have then $t_{v\pm} \propto L_\gamma^{1/2}\Gamma_m^{-5/4} \propto L_\gamma^{(2p-5q)/4p}$. The variability V of the gamma-ray light curves could be expected to scale, in an approximate way, inversely proportional to a power of the minimum variability timescale, $V \propto t_{v,min}^{-k}$. An approximate argument shows that such an anticorrelation exists in the GRB data, with an index $k \simeq 2/3$ (e.g. Ioka & Nakamura 2001; Plaga 2001). Identifying $t_{v,min}$ with $t_{v\pm}$, we have

$$L_\gamma \propto V^{4p/[k(5q-2p)]} \ . \tag{16}$$

If one takes $p = q$, which may be too idealized, the theoretical relation is $L_\gamma \propto V^2$, which is comparable to the lower limit fit of Fenimore & Ramirez-Ruiz (2001); the same result is obtained

for $p = 5/2,\ q = 2,\ k = 1$. Using the nominal values $p = 5/2,\ q = 2,\ k = 2/3$ we get $L_\gamma \propto V^3$, in good agreement with the observed best-fit relation $L_\gamma \propto V^{3.3}$ of Fenimore & Ramirez-Ruiz (2001).

6. Discussion

We have discussed the properties of the quasi-thermal baryonic photospheric radiation component in GRB. At high isotropic equivalent luminosities, this component can dominate the non-thermal shock component, and appears in the hard X-ray range in the source frame. Such sources may be identified with the X-ray excess (Preece *et al.* 1996) class of bursts. This photospheric quasi-thermal component can inverse-Compton cool the non-thermal electrons in the shocks above it, suppressing the MeV synchrotron component and enhancing an inverse-Compton GeV non-thermal component. For high dimensionless entropy $\eta = L/\dot{M}c^2$ and low ($z \lesssim 1$) redshifts the quasi-thermal component appears at hard X-rays (and in extreme cases at γ-rays), whereas for high redshifts (and/or low η) it appears at soft X-rays. We also have identified a new regime in the description of baryonic photospheres from relativistic outflows, which is valid at moderate to high η. The value of the final coasting Lorentz factor of the outflow is not automatically the value it has when the flow becomes optically thin, and has three different possible values $\eta,\ \eta_*^2\eta^{-1/2},\ \eta_*$, as discussed below equation (5), depending on the value of the initial dimensionless entropy η.

We have quantified the location of the outermost radius at which pairs can form in internal shocks, and have argued that highly variable gamma-ray light curves arise mostly from shocks above this limiting pair-shock radius. The pair-shock radius determines the approximate ratio of the fluences in a variable gamma-ray non-thermal component and in a less variable softer ($\gtrsim$ 20-25 keV) X-ray component. The latter could also be responsible for X-ray excess GRB, and, for moderately low bulk Lorentz factors or moderately high redshifts $\Gamma[2/(1+z)] \gtrsim 60$, would be similar to most of the currently known X-ray flash (XRF) bursts (Heise *et al.* 2001; Kippen *et al.* 2001), but additional considerations may be needed to fit naturally the softest (3-5 keV) XRFs. Smoother X-ray components are also obtained from closer-in shocks neglecting pair formation (e.g. Ramirez-Ruiz & Lloyd-Ronning 2002; Spada *et al.* 2000), but smoothing and softening is stronger when there is pair formation (see also Kobayashi *et al.* 2002). This pair X-ray component is generally softer than that of the baryonic photosphere. When present, the pair photosphere enshrouds the baryonic photosphere, but its modest opacity $\tau_\pm \lesssim 3$ is not sufficient to alter significantly the spectrum of the baryonic photosphere. One or both of these X-ray rich components may be present, depending on the bulk Lorentz factor and isotropic equivalent total energy of the burst, and criteria are discussed for the non-thermal γ-ray components to dominate over, or be dominated by, these X-ray components.

An individual burst is characterized in Figure 1 by an average $\eta = (L/\dot{M}c^2)$. The shock radius $r_{sh,o}$ plotted in Figure 1 is for the minimum variability time $t_v = t_o \sim 0.3$ ms, and a second shock radius $r_{sh,3}$ is shown for $t_v = 10^3 t_o \sim 0.3$ s. For $t_v \sim t_o$ and $\eta \lesssim \eta_t$ the corresponding shocks

occur below both the baryonic r_{ph} and pair shock $r_{\pm}$ photospheres, leading to X-ray rich bursts whose variability is partially suppressed. For $t_v \gtrsim 10^3 t_o$ and $\eta \gtrsim \eta_t$ shocks occur at or above both r_{ph} and $r_{\pm}$ leading to hard γ-rays with large variabilty at $\gtrsim 0.3$ s. An individual burst may have several variability timescales present, leading to both types of components simultaneously. Preponderance of one or the other leads to a short timescale but low amplitude variability X-ray rich bursts or XRF, or to a classical hard GRB with large amplitude variability mostly at $\gtrsim 0.3$ s. Roughly speaking, X-ray flashes would be expected from the region $\eta < \eta_t \sim 250$, and classical GRB from $\eta > \eta_t$. A baryonic photosphere component should be present at the begining of bursts and X-ray flashes, and in the troughs between harder peaks due to shock radiation. However, the farther beyond the coasting radius the photosphere occurs, the weaker its energy fraction is relative to the shock and/or $e^{\pm}$ component, because its energy drops as $r^{-2/3}$. Low values of η lead to further-out, weaker baryon photospheres, and at the same time to harder, relatively stronger shocks ocurring closer in to the photosphere. If long variability timescales are absent and $\eta \ll \eta_t$ a soft baryon photosphere may be the most prominent component, but its total energy would be very low. A strong baryonic photosphere dominated burst (with quasi-thermal $\gtrsim$ MeV spectrum) is possible (for shock efficiencies $\lesssim 0.1$) for $\eta \gtrsim \eta_*^{4/3}$, and such a component may be detectable already for $\eta \gtrsim \eta_* \sim 10^3$. On the other hand, slower $\eta \lesssim \eta_t \sim 250$ outflows are likelier to make X-ray rich bursts through a pair-shock component.

We argue also that the relationship between variable gamma-ray radiation and the limiting pair-shock radius leads, using the phenomenologically inferred dependence between isotropic luminosity and jet angle, to a simple analytical interpretation for the observed variability-luminosity relation $L_\gamma \propto V^3$ (e.g. Fenimore and Ramirez-Ruiz 2001; see also Kobayashi *et al.* 2002). The positive correlation between variability and harder νF_ν peaks discussed by Lloyd-Ronning & Ramirez–Ruiz (2002) also finds a qualitatively similar interpretation in terms of a higher variability corresponding to closer-in shocks, which are more specifically in the present model shocks occurring just above the limiting pair-forming shock radius.

Several physical explanations have been proposed for the presence of a cutoff above about 1 Hz in the power density spectrum of GRB light curves (Beloborodov *et al.* 1998) in terms of baryonic electron scattering (e.g. Panaitescu *et al.* 2000; Spada *et al.* 2000; Ramirez-Ruiz & Lloyd-Ronning 2002). Here we point out a different explanation for this, which is based on the existence of a minimum γ-ray variability timescale (equation [10]) above which shock radiation is free from smoothing by opacity from pair-formation. This is seen in Figure 1, which shows that shocks associated with the variability timescales $t_v \gtrsim 1$ s and $\eta \gtrsim 150$ common among observed GRB occur above the pair photosphere.

This research is supported by NASA NAG5-9192, NAG5-9153 and the Royal Society. We are grateful to S. Kobayashi for valuable discussions.

REFERENCES

Beloborodov, A. M., Stern, B. E. & Svensson, R., 1998, ApJ, 508, L25

Fenimore, E. E. & Ramirez-Ruiz, E., 2001, ApJ subm (astro-ph/0004176)

Frail, D., Kulkarni, S., Sari, R., Djorgovski, S., Bloom, J., *et al.* , 2001, ApJ, 562, L55

Ghisellini, G. & Celotti, A., 1999, ApJ, 511, L93

Guilbert, P. W., Fabian, A. C. & Rees, M. J., 1983, MNRAS 205, 593

Heise, J., *et al.* 2000, in *Gamma-Ray Bursts in the Afterglow Era* (astro-ph/0111246)

Ioka, K., & Nakamura, T., 2001, ApJ, 554, L163

Kippen RM, *et al.* , 2001, in *Procs Woods Hole GRB Workshop*, in press (astro-ph/0203114)

Kobayashi, S., Ryde, F., & MacFadyen, A. W., 2002, ApJ, in press (astro-ph/0110080)

Lloyd-Ronning, N. M. & Ramirez-Ruiz, E., 2002, ApJ, in press (astro-ph/0205127)

MacFadyen, A. W., & Woosley, S., 1999. ApJ, 524, 262

Mészáros , P. & Rees, M. J., 2000, ApJ, 530, 292

Norris, J., 2002, ApJ, subm (astro-ph/0201503)

Panaitescu, A., & Kumar, P., 2001, ApJ, 560, L49

Panaitescu, A., Spada, M., & Mészáros , P., 1999, ApJ, 522, L105

Piran, T., Kumar, P., Panaitescu, A. & Piro, L., ApJ, 560, L167

Plaga, R., 2001, A&A, 370, 351

Preece, R., Briggs, M., Pendleton, G., Paciesas, W., Matteson, J., Band, D., Skelton, R. T. & Meegan, C., 1996, ApJ, 473, 310

Preece, R, Briggs, M, Mallozzi, R, Pendleton, G, Paciesas, W, Band, D, 2000, ApJS, 126, 19

Ramirez-Ruiz, E. & Lloyd-Ronning, N. M., 2002, NewA, 7, 197

Ramirez-Ruiz, E., *et al.* , 2002, in preparation

Reichart, D, Lamb, D, Fenimore, EE, Ramirez-Ruiz, E, Cline, T, Hurley, K, 2001, ApJ 552, 57

Rossi, E., Lazzati, D., & Rees, M. J., 2002, MNRAS, 332, 945

Salmonson, J. & Galama, T., 2002, ApJ, 569, 682

Spada, M., Panaitescu, A. & Mészáros , P., 2000, ApJ, 537, 824

Svensson, R., 1987, MNRAS 227, 430

Zhang, B., & Mészáros , P., 2002, ApJ, 571, 876

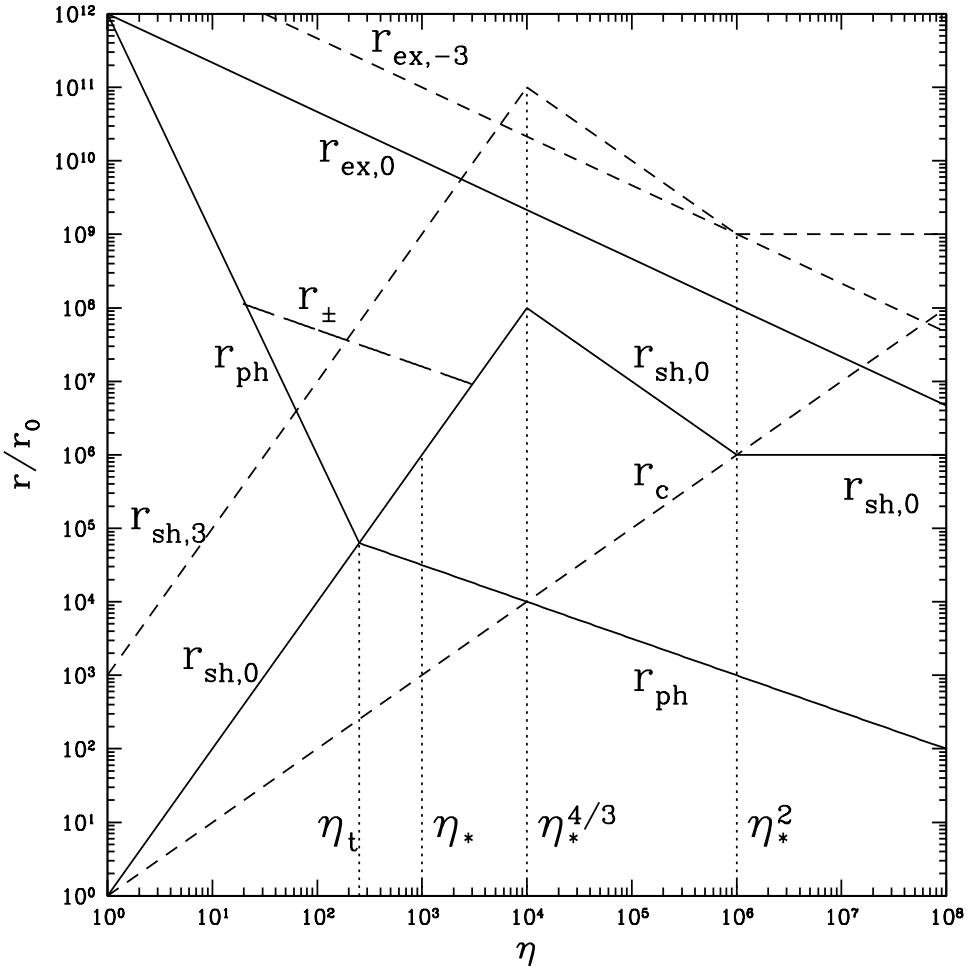

Fig. 1.— Schematic plot of the baryonic photospheric radius r_{ph}; the internal shock radii $r_{sh,o}$, $r_{sh,3}$ for two different variability timescales t_o, $10^3 t_o$ where $t_o = 0.3$ ms; the thin shell pair-producing photospheric radius $r_\pm$; and the thin shell coasting radius r_c starting at $r_o = ct_o$, as a function of $\eta = L/\dot{M}c^2$. Distinguishing between the continuous wind and discrete shell regimes leads to a new characteristic value $\eta_t = \eta_*^{4/5}$ and a distinct regime between η_* and $\eta_*^{4/3}$ (equations (1,4, see text). Shocks can only occur above $r_{sh,o}$, and pair-forming shocks only occur below $r_\pm$. Also shown is the external shock radius for two external densities $n_{ext} = 1, 10^{-3}\mathrm{cm}^{-3}$, giving an upper limit for internal shock radii.